Optimal Control and Control Co-Design of Wind and Marine Turbines Using Derivative Function Surrogate Models

Preliminary Examination

Athul Krishna Sundarrajan[1]

[1] Graduate Student
Department of Systems Engineering
Colorado State University
Athul.Sundarrajan@colostate.edu

December 14, 2023, Fort Collins,
Advisor: Dr. Daniel R. Herber
Committee Members: Dr. James Cale, Dr. Steven Conrad, Dr. Gaofeng Jia

Outline

1. Introduction
2. Background
3. Control of Floating Marine Hydrokinetic Turbines
4. Derivative Function Surrogate Model
5. Additional Results
6. Future Work
7. Appendix

1

Introduction

→ My Background

Education

- 2013 – 2017: B.S. Mechanical Engineering, SASTRA University
- 2019 – 2021: M.S. Systems Engineering, CSU
  - Thesis title: Some Efficient Open-Loop Control Solution Strategies for Dynamic Optimization Problems and Control Co-Design
- 2021 – Present: Ph.D. Systems Engineering, CSU, Fort Collins, CO

Research Experience

- 2018 – 2019: Research Assistant, National Institute of Technology, Trichy
  - Development of bio-inspired vacuum insulation panels (VIP)
- 2020 – Present: Graduate Research Assistant, CSU, Fort Collins, CO
  - Development of open-source tools for lower-order modeling, solution methods for control co-design of Floating Offshore Wind Turbines (FOWT) and Marine Turbines
- Summer 2023: Graduate Intern, National Renewable Energy Laboratory, Boulder, CO
  - Development of an optimal closed-loop blade-pitch controller for marine turbines

→ Design of Dynamic Systems

- Floating offshore wind turbines (FOWTs) and floating marine hydrokinetic turbines can help harvest energy in offshore wind and tidal currents [1]
- The design of dynamic systems like FOWT/marine turbines can be challenging and time-consuming
  - Airfoil shape $\rightarrow$ blade structural properties $\rightarrow$ generator $\rightarrow$ tower, platform, mooring $\rightarrow$ control[2]
  - Controllers are needed to ensure power generation and stability across all environmental conditions
- Computational models are developed for these systems and are used to design them
  - Design optimization is used to identify optimal designs that minimize key performance objectives
- Traditional design process has followed a sequential approach
  - In these systems, there are strong interactions between the structural dynamics and the controller
- The plant and the control must be designed concurrently to obtain system-level optimal designs
- Recently, the importance of formal **integrated design approaches like control co-design (CCD)** have been recognized by experts[3]

[1] Garcia-Sanz 2019b; Garcia-Sanz 2019a; Ross et al. 2022; J. Jonkman et al. 2021 [2] Pao et al. 2021
[3] Garcia-Sanz 2019b

→ Control Co-Design

- Control co-design (CCD) is a class of integrated design methods that **concurrently optimize the dynamic system's physical and control aspects**[1]
- CCD can help overcome some of the limitations of traditional sequential approaches
- CCD has been used to find system-level optimal designs for various dynamic systems
- These results have motivated researchers to use CCD for designs for wind and marine turbines[2]

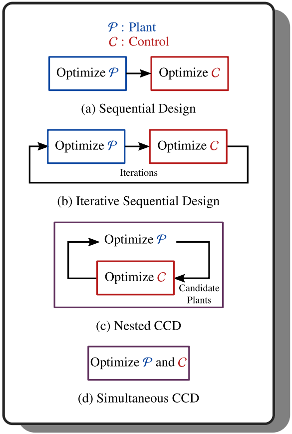

[1] Allison, T. Guo, and Han 2014 [2] Sundarrajan, Hoon Lee, et al. 2023; Ross et al. 2022

→ Optimal Control

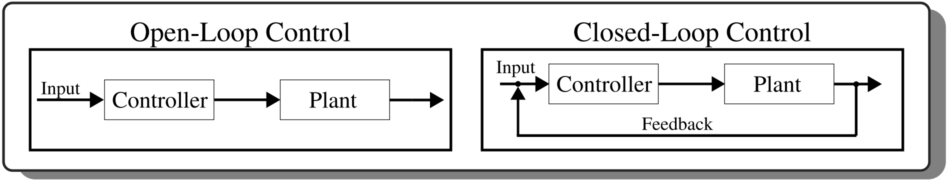

- Optimal control studies are carried out for wind/marine turbines to understand ideal controller behavior
- Two types of control design studies are possible using CCD, namely open-loop and closed-loop

→ Optimal Control (cont.)

- Open-loop optimal control does not assume a particular control architecture, and it can help identify the maximum achievable performance limits
  - But, open-loop control cannot be used to control an actual turbine
- Closed-loop control strategies are needed to design practical control solutions
  - Closed-loop controllers work with limited information
- Because of these reasons, the optimal control results from open-loop and closed-loop studies are different
- Previous studies have used open-loop optimal control-based CCD
  - The design identified using open-loop optimal control-based CCD is predicated on this aspect of open-loop optimal control
- Few studies have investigated approaches to design closed-loop controllers using open-loop optimal control results in the context of CCD

RQ **Identifying suitable strategies to bridge the gap between open-loop and closed-loop-based CCD would be key to utilizing the trade-offs identified using CCD**

→ FOWT Design

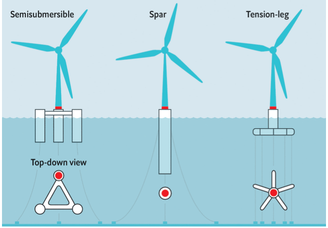

Different platform types for FOWT *Adopted from Ref. Mei and Xiong 2021*.

- Initial design efforts for FOWTs started from the standard onshore configuration[1]
- Studies were carried out to identify stable platform and mooring configurations
  - Three different platform types have been identified: the semisubmersible, the spar buoy, and the tension leg platform (TLP)[2]
- The platform's floating motion affects the dynamics of the FOWT, and these motions are key plant and control design drivers[3]

[1] J. Jonkman 2008; Butterfield et al. 2007 [2] Thiagarajan and Dagher 2014; Butterfield et al. 2007 [3] J. Jonkman 2008; J. M. Jonkman and Matha 2011

→ FOWT Design (cont.)

- Several studies have investigated the application of CCD to FOWTs[1]
  - These studies have shown the importance of including control design to identify stable and optimal platform designs
- But the focus of these studies is for specific platform types
- The choice of support structure for FOWTs is still an open question in industry and academia
- Previous studies have investigated the trade-offs between different platform types [2]
  - The comparisons were made for baseline turbine and platform designs, and the cost is not taken into account
- By comparing the performance of optimal designs, key trade-offs can be understood

RQ **Comparing the performance of optimized FOWT designs identified using CCD will help identify the key design trade-offs and provide a fair comparison**

[1] Abbas, Jasa, et al. 2024; Sundarrajan, Hoon Lee, et al. 2023; Bayat, Lee, and Allison 2023 [2] J. M. Jonkman and Matha 2011; Zalkind et al. 2022

→ Marine Turbine Design

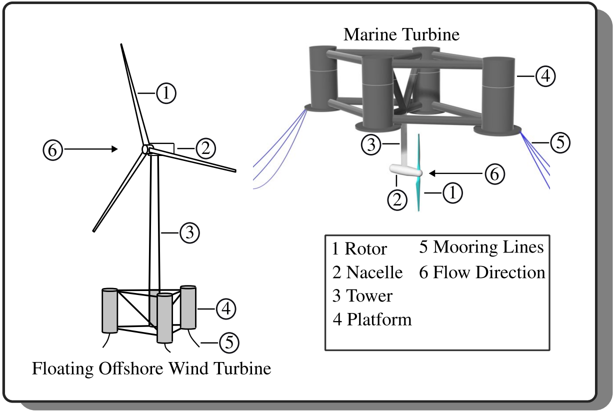

- The principle of operation of marine turbines is similar to that of wind turbines

→ Marine Turbine Design (cont.)

- Unlike wind turbines, there is no consensus on a standard configuration for marine turbines
- Exploring multiple designs and comparing their performance can help in identifying an optimal design that balances multiple considerations
- Marine turbines' current modeling and design practices do not facilitate efficient design space exploration[1]
  - Lower-order models and experimental setups have been used to model, design, and test marine turbines[2]
- These studies provide critical insights, but it is unclear if this approach can be easily extended to other designs and architectures

[1] X. Guo et al. 2018; L. Zhang et al. 2015; Dewhurst et al. 2013; Jesus Henriques et al. 2014 [2] Dewhurst et al. 2013; Jesus Henriques et al. 2014; Martinez et al. 2020; Tatum et al. 2016; Ordonez-Sanchez et al. 2019

→ Marine Turbine Design (cont.)

- OpenFAST, an open-source modeling tool for horizontal-axis wind turbines developed, has been extended to simulate marine turbines[1]
- To simulate a given marine turbine model using OpenFAST, a controller is necessary
  - Currently, there are no controllers for marine turbines that can be directly used with OpenFAST
  - Therefore, a controller needs to be developed
- ROSCO, an open-source controller developed by NREL for wind turbines that has an automated tuning process[2]

RT Extending ROSCO for control of marine turbines would enable CCD of marine turbines

[1] Murray, Thresher, and J. Jonkman 2018 [2] Abbas, Zalkind, et al. 2022

→ Marine Turbine Design (cont.)

- Marine turbines have been deployed in a fixed-bottom configuration
- Researchers have identified the operational benefits of floating marine turbines
  - Lower installation and operational costs[1]
- But a floating configuration would increase the loads, potentially resulting in increased downtime
  - Similar to FOWTs, costs would be higher
- The sequential design approach has been predominantly used for the design of marine turbines
  - But the sequential approach doesn't take into account the effect the controller has on the optimal design
- To show it is possible to find feasible/cost-optimal designs, it is necessary to show that large LCOE reduction is possible using CCD

RQ **Using the CCD approach, identify pathways that could result in a large reduction in the LCOE of floating marine turbine systems using CCD as compared to the sequential approach**

[1] Dewhurst et al. 2013; Fraenkel 2002

→ Issues with Computational Time

- To facilitate all of these studies, computationally inexpensive models of FOWT/marine turbines systems are required
  - Detailed models of these systems can be computationally expensive
- Numerical programming approaches used to solve the design problem can require several hundred function evaluations
- The software architecture of these system models might be such that it is impossible to link all the necessary variables of interest directly to an optimizer
- Several approaches have been studied to overcome this issue:
  1. Develop lower-order models that capture the essential physics of the system[1]
  2. Use linearized models derived from high-fidelity modeling tools[2]
- But these approaches have various drawbacks that limit their use

RT/RQ **Construct surrogates of the dynamic model that can be used in CCD studies**

[1] Bayat, Lee, and Allison 2023 [2] Sundarrajan, Hoon Lee, et al. 2023

→ Research Questions

Summarizing the previous sections, the research goals and tasks explored in this dissertation are as follows:

- RQ1 Using the CCD approach, identify pathways that could result in a large reduction in the LCOE of floating marine turbine systems
- RQ2 Identify the trade-offs between different platform designs for FOWTs using CCD
- RQ3 Identify approaches to construct closed-loop optimal controllers based on the insights identified using open-loop optimal control trajectories

In order to answer these research questions, the following tasks need to be completed:

- RT1 Develop an easy-to-tune controller that can be used for closed-loop control of marine turbines[1]
- RT2 Identify an approach to construct computationally inexpensive surrogate models of FOWT and marine turbine systems that can be used for both open-loop and closed-loop optimal control-based CCD studies[2]

[1] Sundarrajan, Daniel R. Herber, et al. 2024 [2] Sundarrajan and Herber 2023

2

Background

→ WEIS Toolbox

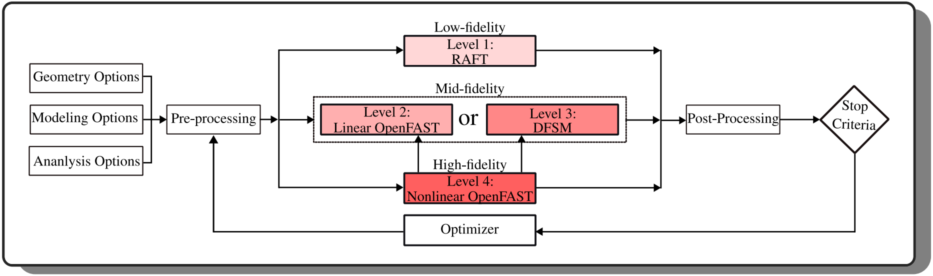

- The motivating application is to create a state-of-the-art wind and marine turbine design tool named WEIS[1]
- It is built on OpenFAST[2] and can perform CCD studies at three different levels of fidelity
- The pre and post-processing blocks have different modules that can estimate the cost and levelized cost of energy (LCOE) for wind and marine turbines

[1] J. Jonkman et al. 2021 [2] *OpenFAST* n.d.

→ Simultaneous CCD Formulation

$$
\begin{aligned}
\underset{\boldsymbol{u},\boldsymbol{\xi},\boldsymbol{x}_p}{\text{minimize:}} \quad & o = \mathcal{M}(\boldsymbol{\xi}(t_0), \boldsymbol{\xi}(t_f), \boldsymbol{x}_p) + \int_{t_0}^{t_f} \mathcal{L}(t, \boldsymbol{u}, \boldsymbol{\xi}, \boldsymbol{y}, \boldsymbol{x}_p) dt && \text{(1a)} \\
\text{subject to:} \quad & \dot{\boldsymbol{\xi}}(t) - \boldsymbol{f}(t, \boldsymbol{u}, \boldsymbol{\xi}, \boldsymbol{x}_p) = \boldsymbol{0} && \text{(1b)} \\
& \boldsymbol{\mathcal{P}_h}(t, \boldsymbol{u}, \boldsymbol{\xi}, \boldsymbol{y}, \boldsymbol{x}_p) = \boldsymbol{0} && \text{(1c)} \\
& \boldsymbol{\mathcal{P}_g}(t, \boldsymbol{u}, \boldsymbol{\xi}, \boldsymbol{y}, \boldsymbol{x}_p) \leq \boldsymbol{0} && \text{(1d)} \\
& \boldsymbol{\mathcal{B}_h}(t_0, t_f, \boldsymbol{\xi}(t_0), \boldsymbol{\xi}(t_f)) = \boldsymbol{0} && \text{(1e)} \\
& \boldsymbol{\mathcal{B}_g}(t_0, t_f, \boldsymbol{\xi}(t_0), \boldsymbol{\xi}(t_f)) \leq \boldsymbol{0} && \text{(1f)} \\
\text{where:} \quad & \boldsymbol{y} = \boldsymbol{g}(t, \boldsymbol{u}, \boldsymbol{\xi}, \boldsymbol{x}_p)
\end{aligned}
$$

- $t \in [t_0, t_f]$ is the defined time horizon
- $\boldsymbol{\xi}$: states (e.g., generator speed and platform pitch)
- $\boldsymbol{u}$: controls (e.g., generator torque and the blade pitch)
- $\boldsymbol{x}_p$: plant variables (e.g., tower height and thickness, blade length, platform mass)
- $\boldsymbol{y}$: outputs (e.g., generator power , blade and tower loads)

→ Simultaneous CCD Formulation (cont.)

$$
\begin{aligned}
\underset{\boldsymbol{u},\boldsymbol{\xi},\boldsymbol{x}_p}{\text{minimize:}} \quad & o = \mathcal{M}(\boldsymbol{\xi}(t_0), \boldsymbol{\xi}(t_f), \boldsymbol{x}_p) + \int_{t_0}^{t_f} \mathcal{L}(t, \boldsymbol{u}, \boldsymbol{\xi}, \boldsymbol{y}, \boldsymbol{x}_p)dt && \text{(2a)} \\
\text{subject to:} \quad & \dot{\boldsymbol{\xi}}(t) - \boldsymbol{f}(t, \boldsymbol{u}, \boldsymbol{\xi}, \boldsymbol{x}_p) = \boldsymbol{0} && \text{(2b)} \\
& \boldsymbol{\mathcal{P}}_{\boldsymbol{h}}(t, \boldsymbol{u}, \boldsymbol{\xi}, \boldsymbol{y}, \boldsymbol{x}_p) = \boldsymbol{0} && \text{(2c)} \\
& \boldsymbol{\mathcal{P}}_{\boldsymbol{g}}(t, \boldsymbol{u}, \boldsymbol{\xi}, \boldsymbol{y}, \boldsymbol{x}_p) \leq \boldsymbol{0} && \text{(2d)} \\
& \boldsymbol{\mathcal{B}}_{\boldsymbol{h}}(t_0, t_f, \boldsymbol{\xi}(t_0), \boldsymbol{\xi}(t_f)) = \boldsymbol{0} && \text{(2e)} \\
& \boldsymbol{\mathcal{B}}_{\boldsymbol{g}}(t_0, t_f, \boldsymbol{\xi}(t_0), \boldsymbol{\xi}(t_f)) \leq \boldsymbol{0} && \text{(2f)} \\
\text{where:} \quad & \boldsymbol{y} = \boldsymbol{g}(t, \boldsymbol{u}, \boldsymbol{\xi}, \boldsymbol{x}_p)
\end{aligned}
$$

- $\mathcal{M}(\boldsymbol{\xi}(t_0), \boldsymbol{\xi}(t_f), \boldsymbol{x}_p)$: Mayer term or terminal cost
- $\mathcal{L}(t, \boldsymbol{u}, \boldsymbol{\xi}, \boldsymbol{x}_p)$: Lagrange term or running cost (e.g., maximize captured power)
- $\boldsymbol{f}(t, \boldsymbol{u}, \boldsymbol{\xi}, \boldsymbol{x}_p)$: dynamic function or the state derivative function
- $\boldsymbol{g}(t, \boldsymbol{u}, \boldsymbol{\xi}, \boldsymbol{x}_p)$: output function
- $\boldsymbol{\mathcal{H}} = \{\boldsymbol{\mathcal{P}}_{\boldsymbol{h}}, \boldsymbol{\mathcal{B}}_{\boldsymbol{h}}\}$: set of equality path and boundary constraints (e.g., initial values of the states or control variables)
- $\boldsymbol{\mathcal{G}} = \{\boldsymbol{\mathcal{P}}_{\boldsymbol{g}}, \boldsymbol{\mathcal{B}}_{\boldsymbol{g}}\}$: set of inequality path and boundary constraints (e.g., simple state and control bounds, limitation on the tower bending moment)

→ Closed-Loop CCD formulation

- We consider a closed-loop CCD problem where the plant variables ($\boldsymbol{x}_p$) and controller parameters ($\boldsymbol{x}_u$) are the design variables

$$\begin{aligned}
\underset{\boldsymbol{x}_u,\boldsymbol{x}_p}{\text{minimize:}} \quad & o(\boldsymbol{u},\boldsymbol{\xi},\boldsymbol{y},\boldsymbol{x}_p) && \text{(3a)}\\
\text{subject to:} \quad & \boldsymbol{\mathcal{H}}(t,\boldsymbol{u},\boldsymbol{\xi},\boldsymbol{y},\boldsymbol{x}_p,\boldsymbol{\xi}(t_0),\boldsymbol{\xi}(t_f)) = \boldsymbol{0} && \text{(3b)}\\
& \boldsymbol{\mathcal{G}}(t,\boldsymbol{u},\boldsymbol{\xi},\boldsymbol{y},\boldsymbol{x}_p,\boldsymbol{\xi}(t_0),\boldsymbol{\xi}(t_f)) \leq \boldsymbol{0} && \text{(3c)}\\
\text{where:} \quad & \boldsymbol{u} = \boldsymbol{C}(\boldsymbol{x}_u,\boldsymbol{\xi})\\
& \boldsymbol{\xi} = \int_{t_0}^{t_f} \dot{\boldsymbol{\xi}}(t)\mathrm{d}t = \int_{t_0}^{t_f} \boldsymbol{f}(t,\boldsymbol{u},\boldsymbol{\xi},\boldsymbol{x}_p)\mathrm{d}t\\
& \boldsymbol{y} = \boldsymbol{g}(t,\boldsymbol{u},\boldsymbol{\xi},\boldsymbol{x}_p)
\end{aligned}$$

- $\boldsymbol{C}(\boldsymbol{x}_u,\boldsymbol{\xi})$ is the controller
- $\int_{t_0}^{t_f} \dot{\boldsymbol{\xi}}(t)\mathrm{d}t$ is solved using an ODE solver

→ Solution Strategies

- The problem variables, and solution strategies are different for both open-loop and closed-loop problems
    - Open-loop optimal control/CCD problems require the solution of $\boldsymbol{u}(t)$ at every instance in t
    - Closed-loop problems require the solution of the plant variables and controller parameters, which are not time-varying
- We use the direct transcription (DT) method to solve open-loop CCD problems and a shooting-based approach to solving closed-loop CCD problems
- Shooting-based approaches are less intrusive
    - The optimizer generates candidate solutions
    - The system is simulated for these candidates using an ODE solver
    - The constraints and objectives are measured from the simulations
- DT approaches are more intrusive and need information about the dynamic model
    - The given time horizon is discretized into n_t nodes
    - The control and state values at each point in time is an optimization variable
    - The dynamics are enforced as constraints between the discretized points

$$\boldsymbol{\xi}_{i+1} = \boldsymbol{\xi}_i + \frac{1}{2}h(\boldsymbol{f}_i(\cdot) + \boldsymbol{f}_{i+1}(\cdot))$$

→ Solution Strategies

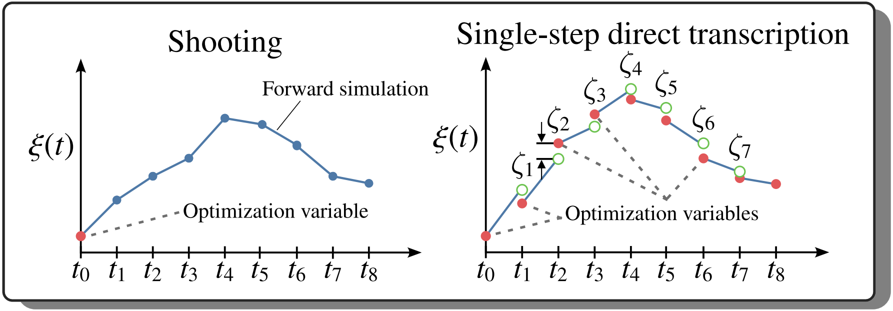

- Both these approaches are used to solve the different open-loop/closed-loop problems
- The surrogate modeling approach must be applicable with both these methods

3

Development of an Optimal Variable Pitch Controller for Floating Axial-Flow Marine Hydrokinetic Turbines

→ Motivation

- Controller design practices for marine turbines have been adopted from wind turbine literature
  - Linearized models are obtained around set operating points, and controllers are designed through Bode-shaping[1]
  - The expertise of a control engineer is needed to identify optimal gains
- This approach can be time-consuming and harder to automate
  - Does not enable efficient design space exploration
- Reference open source controller (ROSCO) was developed to particularly address this issue
- ROSCO has an automated tuning process while providing industry-standard functionalities
  - ROSCO can be coupled with an optimizer to identify the optimal parameters ($\boldsymbol{x}_c$)
- ROSCO is an ideal tool to be used in early-stage design studies

[1] Gunnink 2015

→ Control-Loops

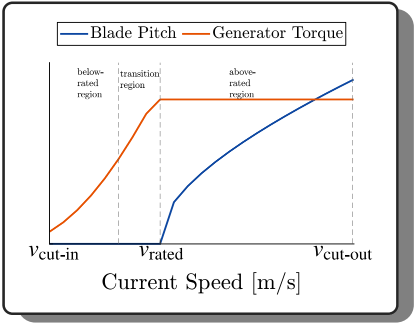

- The generator torque (τ_g) and the blade pitch angle (β) are the two main control variables for wind and marine turbines
- The operating region is separated into three different regions
  - Below-rated (BR), transition (TR) and above-rated (AR)
- Different control goals and variables are used in these regions
  - BR - Generator torque, TR - combination of both, AR - blade pitch

→ ROSCO Overview

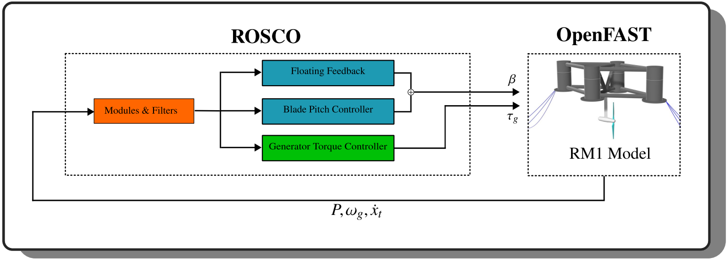

- There are two primary control loops for τ_g and β
- A Proportional-Integral (PI) architecture is used for both controllers
- The main feedback variables are the generator speed (ω_g), generator power (P), and tower-top velocity ($\dot{x}_t$)
- The input to this closed-loop system is the generator speed error, measured as:

$$-\Delta\omega_g = \omega_{g,\mathrm{ref}} - \omega_g \tag{4}$$

- Different $\omega_{g,\mathrm{ref}}$ are used for both controllers

→ ROSCO Overview (cont.)

- ROSCO uses a simplified, first-order model along with the C_p surface of the given turbine to estimate how ω_g varies with τ_g and β:

$$\dot{\omega}_g = \frac{N_g}{J}\left(\tau_a - N_g \tau_g \eta_{\text{gb}}\right) \tag{5a}$$

$$\tau_a = \frac{1}{2}\rho A_r \frac{C_p(\lambda, \beta)}{\omega_r} v^3 \tag{5b}$$

  - These equations can be used to model the relevant aspects of the RM1 turbine too
- The corresponding proportional ($\boldsymbol{k}_p$) and integral ($\boldsymbol{k}_i$) gain schedules for both controllers are derived using first-order linearizations of Eq. (5)
- The closed-loop system between $\Delta\tau_g$ or $\Delta\beta$ and $\Delta\omega_g$ is a second-order system whose response can be characterized by its natural frequency (ω_{des}) and damping ratio (ζ_{des})[1]:

$$H(s) = \frac{\omega_{\text{des}}^2}{s^2 + 2\omega_{\text{des}}\zeta_{\text{des}} + \omega_{\text{des}}^2} \tag{6}$$

- Controller response can be optimized by selecting appropriate values of $[\omega_{\text{des}}, \zeta_{\text{des}}]$

[1] Franklin, Powell, and Emami-Naeini 2015

→ Below-Rated Controller

- The generator torque is the main control variable used in the below-rated region
- The $\omega_{g,\text{ref}}$ used in this region can be obtained as:

$$\tau_g = K\omega_g^2 \quad \text{and} \quad \tau_g = \frac{P}{\omega_g} \tag{7}$$

$$\omega_{g,\text{ref}} = \omega_g = \left[\frac{P}{K}\right]^{\frac{1}{3}} \tag{8}$$

- The values of ω_{vs} and ζ_{vs} are then selected as $\boldsymbol{p}_{\text{vs}} = [0.7, 0.7]$ to derive $\boldsymbol{k}_{p,\text{vs}}$ and $\boldsymbol{k}_{i,\text{vs}}$

→ Above-Rated Controller

- Blade pitch is the main control variable used in the above-rated region
- The control goal in the above-rated region is to track the rated generator speed $\omega_{g,\mathrm{ref}} = \omega_{g,\mathrm{rated}}$
- To improve the performance of the blade pitch controller, multiple values of $\boldsymbol{\omega}_{\mathrm{pc}}$ and $\boldsymbol{\zeta}_{\mathrm{pc}}$ for different values of $\boldsymbol{v}$ can be selected[1]
  - Two values of the current speed v = [2.3,2.5] are used here
- For floating turbines, a feedback term is added to the blade pitch controller response to address the negative-damping problem:
  - This phenomenon occurs as a result of the coupling between the tower motion and the blade pitch
- To counteract this, the tower-top velocity ($\dot{x}_t$) is filtered and proportionally fed back to the blade pitch controller to dampen the pitching motion with a gain $k_{\beta,\mathrm{float}}$
- Several filters are applied to the tower-top velocity signal, and ω_{ptfm} is a key corner frequency that affects the performance of the floating feedback

[1] Zalkind et al. 2022

→ Controller Optimization

- The performance of the blade pitch controller is critical to the turbine design
  - An optimizer is used to identify the key controller parameters
- The performance of the blade pitch controller is characterized by $\boldsymbol{x}_u = [\boldsymbol{\omega}_{\mathrm{pc}}, \boldsymbol{\zeta}_{\mathrm{pc}}, k_{\beta,\mathrm{float}}, \omega_{\mathrm{ptfm}}]$
- A key goal is to minimize the tower-base loads for floating turbines
  - The damage equivalent load for the tower base moment is the objective (DEL_t)
- A constraint is added to limit ω_g to 20% of its rated value
- The resulting optimization problem formulation is:

$$\min_{\boldsymbol{x}_u} \quad \mathrm{DEL}_t \tag{9a}$$

$$\text{subject to:} \quad \omega_g \leq 1.2\omega_{g,\mathrm{rated}} \tag{9b}$$

$$\boldsymbol{x}_{u,\min} \leq \boldsymbol{x}_u \leq \boldsymbol{x}_{u,\max} \tag{9c}$$

where $\boldsymbol{x}_{u,\min} = [0.1, 0.1, -2, 10^{-5}]$ and $\boldsymbol{x}_{u,\max} = [1.5, 3.0, 0.0, 1.0]$ respectively

- A derivative-free optimizer `COBYLA` is used in this study
- The shooting approach is used to solve the problem
  - We simulate the model using fifteen different cases with $v \in [0.5, 4]$ [m/s] from DLC 1.1 for $t = 300$ [s] to calculate DEL_t

→ Results

Table: Optimization results.

Variable	Initial Value ($\boldsymbol{x}_{u,\text{init}}$)	Optimal Value ($\boldsymbol{x}_{u,\text{opt}}$)
$\boldsymbol{\omega}_{\text{pc}}$ [rad/s]	$[0.90, 0.90]$	$[0.67, 0.92]$
ζ_{pc} [-]	$[0.70, 0.70]$	$[0.94, 1.55]$
$k_{\beta,\text{float}}$ [-]	-0.38	-0.43
ω_{ptfm} [rad/s]	0.66	0.41
DEL_t [kNm]	551.32	392.40

- The problem is formulated and solved using the WEIS toolbox, where Level 4 Nonlinear OpenFAST is used to model the dynamic response
- The problem is started from $\boldsymbol{x}_{u,\text{init}}$, and the parameters were identified manually to give a 'reasonable' performance
- The optimizer converges in 50 iterations for a specified tolerance of $o = 10^{-2}$
- There is a 28% reduction in DEL_t between the initial and final values
- Each iteration takes around 5 hours to complete

Results (cont.)

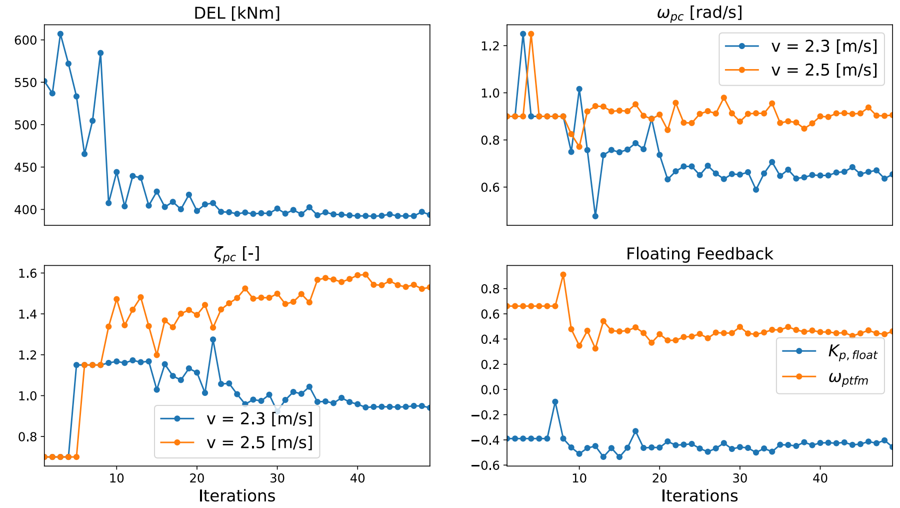

→ Results (cont.)

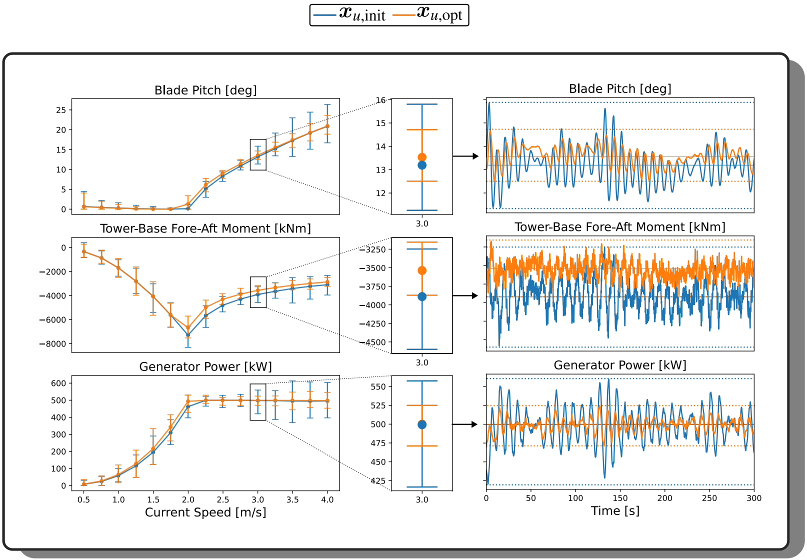

→ Results (cont.)

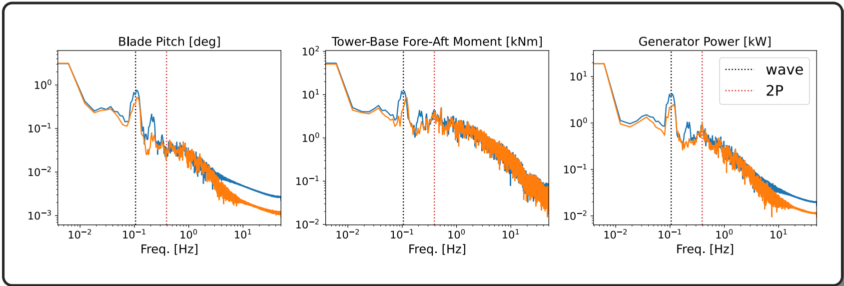

- Lowering ω_{pc} in the near-rated region helps offset the effects of the negative damping problem

---

- The key takeaway is that ROSCO has been extended for control of marine turbines, and by coupling ROSCO with an optimizer, the performance can be improved

4

Constructing Surrogate Models of Wind and Marine Turbines for use in Control and Optimization

→ Introduction

- As seen in the previous study, using detailed wind/marine turbine models directly in design studies can be computationally expensive
  - For efficient design space exploration, inexpensive system models are required
- Surrogate-based design optimization studies typically approximate the input-output response for expensive systems
  - $\boldsymbol{x}_c \rightarrow \mathrm{DEL}_t$ as seen in the previous study
- For dynamic systems, the evolution of the controls and states over the given time horizon is an important consideration
  - The dynamic response must be studied to understand the optimal behavior
- Evaluating this response is sometimes the most computationally expensive operation
- Creating a surrogate model for this would significantly lower the computational expense

→ Derivative Function Surrogate Models

DFSM

$$\dot{\boldsymbol{\xi}} = \boldsymbol{f}(\boldsymbol{u}, \boldsymbol{\xi}) \approx \hat{\boldsymbol{f}}(\boldsymbol{u}, \boldsymbol{\xi}) \tag{10a}$$

$$\boldsymbol{y} = \boldsymbol{g}(\boldsymbol{u}, \boldsymbol{\xi}) \approx \hat{\boldsymbol{g}}(\boldsymbol{u}, \boldsymbol{\xi}) \tag{10b}$$

- We consider the case where the dynamic response can be modeled using ODEs as shown in Eq. (10)
  - This function is referred to as the derivative function
- Creating a surrogate model of this function has been studied under the term **derivative function surrogate model (DFSM)**[1]
- The DFSM provides the state derivative ($\dot{\boldsymbol{\xi}}$) values for given inputs $(\boldsymbol{u}, \boldsymbol{\xi})$
- The steps involved in the construction are:
  - Create a sampling scheme for the inputs $\boldsymbol{I} = (\boldsymbol{u}, \boldsymbol{\xi})$
  - Evaluate the derivative function $\boldsymbol{O} = \boldsymbol{f}(\boldsymbol{I})$
  - Train a surrogate model that maps $\boldsymbol{I} \rightarrow \boldsymbol{O}$
- Once constructed, the DFSM can be used for open-loop or closed-loop optimal control/CCD studies

[1] Deshmukh and Allison 2017; Lefebvre, Belie, and Crevecoeur 2018; Q. Zhang, Wu, and Lu 2022

Caveats

1. Previous studies have assumed direct access to the derivative function
   - But this is not the case with WEIS
2. Prior information about linear model structure has not been used in the construction of the model
   - Some state derivatives ($\dot{\boldsymbol{\xi}}$) can be linear relations of inputs $(\boldsymbol{u}, \boldsymbol{\xi})$. For example:

$$\dot{\xi}_3 = \xi_2 - \xi_1 \quad \text{or} \quad \dot{\xi}_1 = \xi_3$$

3. Limited efforts have been made to validate the model once constructed
   - Model refinement schemes have been used to identify the optimal results
4. Key outputs $(\boldsymbol{y})$ are not captured by the model
   - When designing FOWT, quantities such as tower base force/moment and generated power are important

→ Overview

DFSM

$$f(\cdot) \approx \hat{f}_{low}(\cdot) + e(\cdot) \tag{11}$$

- The goal is to construct a multi-fidelity DFSM model with the structure mentioned above
  - $\hat{f}_{\text{low}}(\cdot)$ is a low-fidelity linear-fit model
  - $e(\cdot)$ is a higher-fidelity component that attempts to approximate the remaining error
- The derivative function in Eq. (10) cannot be evaluated directly, but a black box code can be simulated for a given input $u \in \mathbb{R}^{n_u}$ to get the corresponding outputs $y \in \mathbb{R}^{n_y}$.
- The states $\xi \in \mathbb{R}^{n_\xi}$ are available from the outputs of the simulation y, and the model does not have any other internal states, such that $\xi \subset y$.

→ Steps Involved

1. Run the necessary simulations to obtain the baseline data for state and output trajectories
2. Construct at least a C^1 continuous polynomial approximation of the state trajectories $\hat{\boldsymbol{\xi}}(t)$ and then evaluate polynomial approximation derivative $\dot{\hat{\boldsymbol{\xi}}}(t)$
3. Using the input-output data, construct a least-squares linear-fit approximation creating $\hat{\boldsymbol{f}}_{\text{low}}$
4. Using the input-output data, evaluate the remaining error between the actual state derivatives and the linear-fit model
5. Train a nonlinear surrogate model on this error using a selected approach determining $\boldsymbol{e}$
6. Validate the resulting multi-fidelity model

→ Step 1

Step (1)

Run the necessary simulations to obtain the baseline data for state and output trajectories

- For a given system we generate total of n_{sim} simulations for different control inputs $\boldsymbol{u}$ to get the corresponding outputs $\boldsymbol{y}(t)$
- From $\boldsymbol{y}$, the state trajectories $\boldsymbol{\xi}$ can be extracted and organized as:

$$\boldsymbol{T} = \begin{bmatrix} \boldsymbol{t}^{(1)} & \boldsymbol{t}^{(2)} & \cdots & \boldsymbol{t}^{(n_{\text{sim}})} \end{bmatrix} \tag{12a}$$

$$\boldsymbol{I} = \begin{bmatrix} \boldsymbol{U} \\ \boldsymbol{X} \end{bmatrix} = \begin{bmatrix} \boldsymbol{u}^{(1)} & \boldsymbol{u}^{(2)} & \cdots & \boldsymbol{u}^{(n_{\text{sim}})} \\ \boldsymbol{\xi}^{(1)} & \boldsymbol{\xi}^{(2)} & \cdots & \boldsymbol{\xi}^{(n_{\text{sim}})} \end{bmatrix} \tag{12b}$$

→ Step 2

Step (2)

Construct at least a C^1 continuous polynomial approximation of the state trajectories $\hat{\boldsymbol{\xi}}(t)$ and then evaluate polynomial approximation derivative $\hat{\dot{\boldsymbol{\xi}}}(t)$

- Construct a cubic-spline interpolation scheme for $\boldsymbol{\xi}(t)$ on t
- Cubic-spline interpolation scheme can provide continuous first and second derivatives

$$\dot{\boldsymbol{X}} = \begin{bmatrix} \dot{\boldsymbol{\xi}}^{(1)} & \dot{\boldsymbol{\xi}}^{(2)} & \cdots & \dot{\boldsymbol{\xi}}^{(n_{\text{sim}})} \end{bmatrix} \quad (13)$$

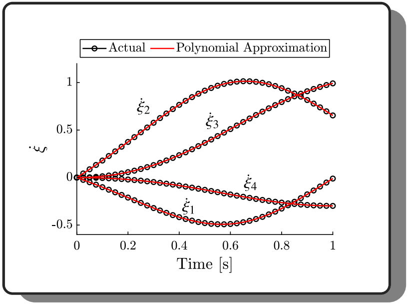

→ Step 3

Step (3)

Using the input-output data, construct a least-squares linear-fit approximation creating $\hat{\boldsymbol{f}}_{low}$

- The low-fidelity portion is found by constructing a least-squares approximation between the inputs $\boldsymbol{I}$ and the state derivatives $\dot{\boldsymbol{X}}$:

$$\hat{\boldsymbol{f}}_{\text{low}}(\boldsymbol{I}) = \hat{\boldsymbol{f}}_{\text{L}}(\boldsymbol{I}) = \boldsymbol{L}\boldsymbol{I} \tag{14a}$$

$$\boldsymbol{L} = (\boldsymbol{I}\boldsymbol{I}^T)^{-1}\boldsymbol{I}^T\dot{\boldsymbol{X}} \tag{14b}$$

- If the system can be characterized by additional parameters $\boldsymbol{w}$, then a LPV system can be constructed as:

$$\hat{\boldsymbol{f}}_{\text{L}} = \boldsymbol{L}(\boldsymbol{w})\boldsymbol{I} = \begin{bmatrix}\boldsymbol{B}_{\text{L}}(\boldsymbol{w}) & \boldsymbol{A}_{\text{L}}(\boldsymbol{w})\end{bmatrix}\boldsymbol{I} \tag{15}$$

→ Step 4

Step (4)

Using the input-output data, evaluate the remaining error between the actual state derivatives and the linear-fit model

- Before constructing the corrective function $\boldsymbol{e}(\cdot)$, it is necessary to subsample from the evaluated error:

$$\boldsymbol{E} = \dot{\boldsymbol{X}} - \boldsymbol{L}\boldsymbol{I} \quad (16)$$

- It is computationally expensive to construct a model using all the data
- We use the k-means method to extract the subsamples

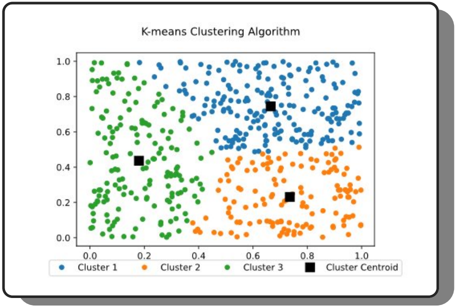

→ Step 5

Step (5)

Train a nonlinear surrogate model on this error using a selected approach determining $\boldsymbol{e}$

- Radial basis functions (RBFs) are used to construct the nonlinear error corrective function $\boldsymbol{e}$ in this study:

$$F(\boldsymbol{x}) = \sum_{i=1}^{N} w_i \cdot \phi(\|\boldsymbol{x} - \boldsymbol{x}_i\|_2) \tag{17a}$$

$$\phi(\boldsymbol{x}) = \exp(-\boldsymbol{x}^2) \tag{17b}$$

→ Step 6

- The sequence of steps can be repeated to get a surrogate model for the outputs $\boldsymbol{y}$

Step (6)

$$\dot{\boldsymbol{\xi}} \approx \hat{\boldsymbol{f}} = \boldsymbol{A}\boldsymbol{\xi} + \boldsymbol{B}\boldsymbol{u} + \boldsymbol{e}_f(\boldsymbol{\xi}, \boldsymbol{u}) \tag{18a}$$

$$\boldsymbol{y} \approx \hat{\boldsymbol{g}} = \boldsymbol{C}\boldsymbol{\xi} + \boldsymbol{D}\boldsymbol{u} + \boldsymbol{e}_g(\boldsymbol{\xi}, \boldsymbol{u}) \tag{18b}$$

→ FOWT Model

- We use the IEA-15 MW FOWT model with a semi-submersible platform
- The main input to the system is the wind speed (w)
- The main states are the platform pitch (Θ_p), generator speed (ω_g), and their first time derivatives ($\dot{\Theta}_p, \dot{\omega}_g$)

$$\boldsymbol{\xi} = [\Theta_p, \omega_g, \dot{\Theta}_p, \dot{\omega}_g]^T \tag{19}$$

$$\dot{\boldsymbol{\xi}} = [\dot{\Theta}_p, \dot{\omega}_g, \ddot{\Theta}_p, \ddot{\omega}_g]^T \tag{20}$$

- The controls are the generator torque (τ_g) and the blade pitch (β)

$$\boldsymbol{u} = [\tau_g, \beta]^T \tag{21}$$

- The tower base fore-aft shear force (T_F) and side-to-side moment (T_M) are the outputs considered

$$\boldsymbol{y} = [T_F, T_M]^T \tag{22}$$

- System simulations are obtained for ten different trajectories from DLC 1.1
- 80% are used to train the DFSM model, and the rest are used for testing

→ Problem Formulation

- An optimal control problem is formulated to maximize the power produced
- Power generation vs. load reduction is a key trade-off in wind turbine design

Problem Formulation

$$\underset{\boldsymbol{u},\boldsymbol{\xi}}{\textit{min:}} \int_{t_0}^{t_f} \left[(-\tau_g \omega_g) + \boldsymbol{u}^T \boldsymbol{W} \boldsymbol{u} \right] \mathrm{d}t \tag{23a}$$

$$\textit{sub to: } \dot{\boldsymbol{\xi}} = \hat{\boldsymbol{f}}(w, \boldsymbol{u}, \boldsymbol{\xi}) \tag{23b}$$

$$\boldsymbol{y} = \hat{\boldsymbol{g}}(w, \boldsymbol{u}, \boldsymbol{\xi}) \tag{23c}$$

$$\boldsymbol{\xi}_{\min} \leq \boldsymbol{\xi} \leq [\Theta_{p,\max}, 7.2] \tag{23d}$$

$$\Theta_{p,\max} = [5, 7] \quad \textit{[deg]}$$

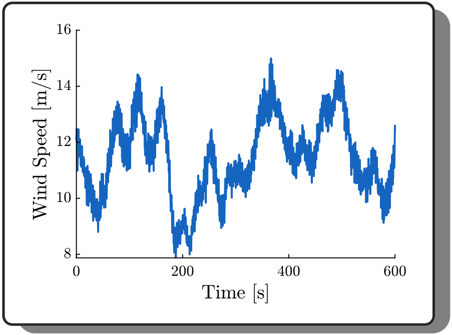

→ Validation

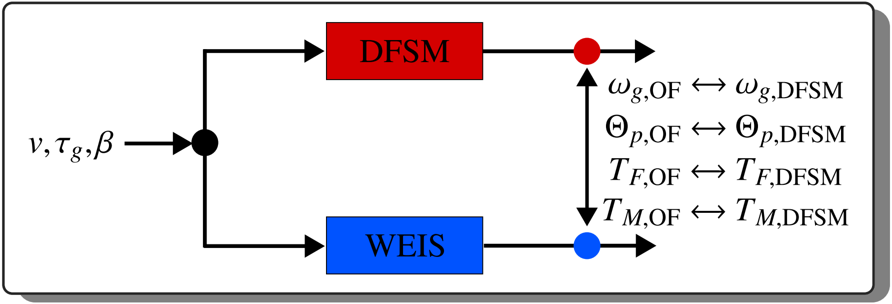

- The DFSM is validated by comparing the simulated states against the results from OpenFAST for the same set of control inputs
- The results are shown for one of the test trajectories in the transition region

→ Validation Results

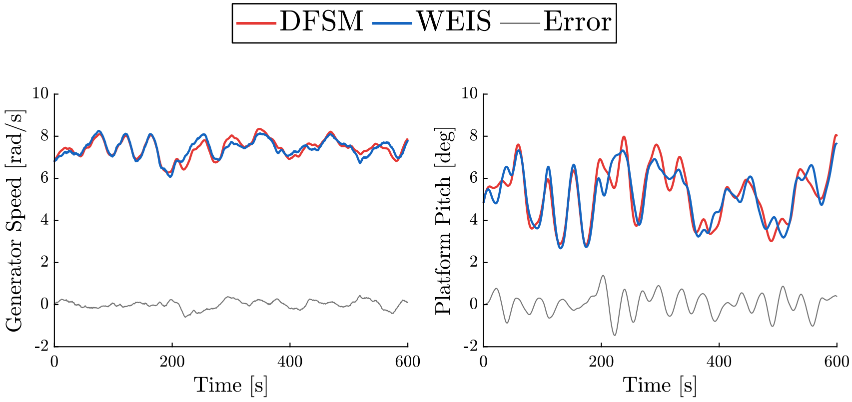

(a) Generator Speed. (b) Platform Pitch.

WEIS simulation time: 20 minutes, **DFSM simulation time**: 4 minutes

→ Validation Results (Cont.)

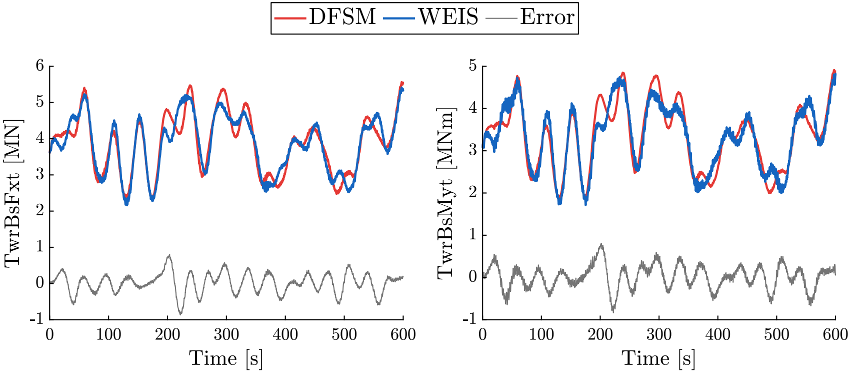

(a) Tower-base shear force.

(b) Tower-base shear moment.

WEIS simulation time: 20 minutes, **DFSM simulation time**: 4 minutes

→ Validation Results (Cont.)

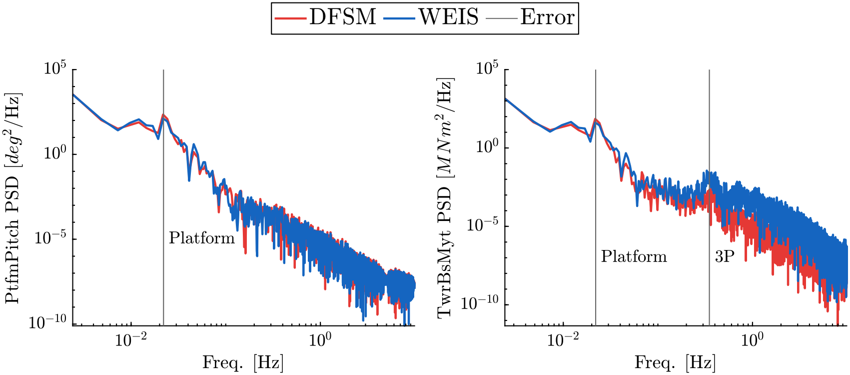

(a) PSD of platform pitch.

(b) PSD of tower-base shear moment.

The PSD shows that the DFSM model can capture the key frequencies.

→ Optimal Controls

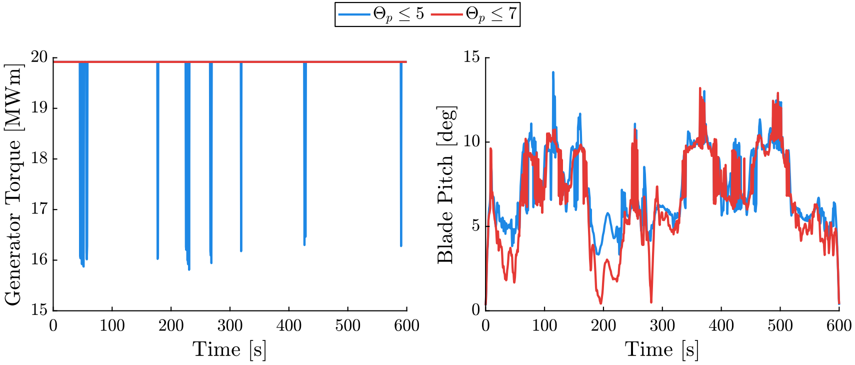

(a) Optimal τ_g. (b) Optimal β.

The trends seen in the optimal control results match common trends seen for wind turbine control.

→ Optimal States

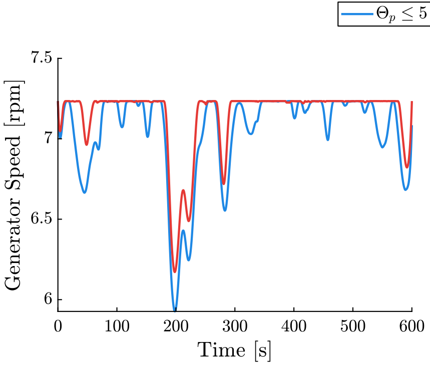

(a) Optimal ω_g.

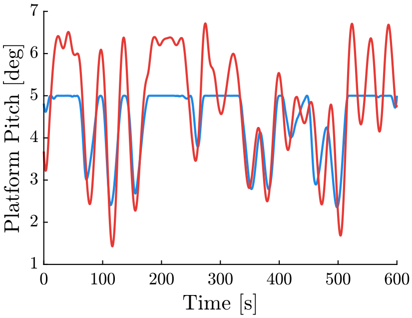

(b) Optimal Θ_p.

The optimizer is able to find solutions that balance the different trade-offs using the DFSM.

→ Outputs

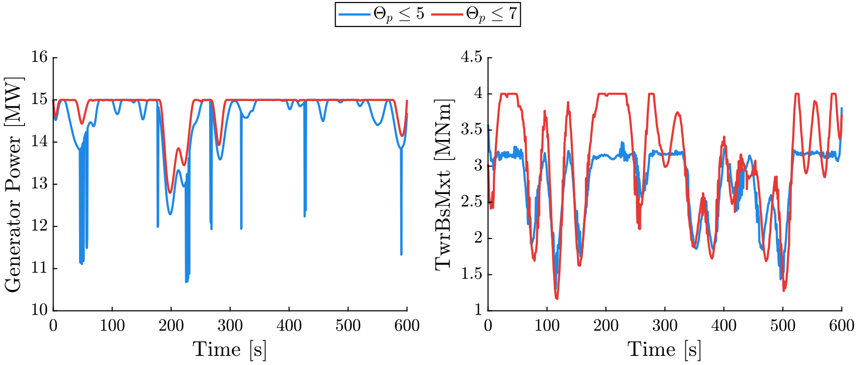

(a) Optimal P.

(b) Optimal T_M.

These figures show the constraint satisfaction v.s. power generation trade-offs.

5

Additional Results

→ ROSCO Simulation Using DFSM

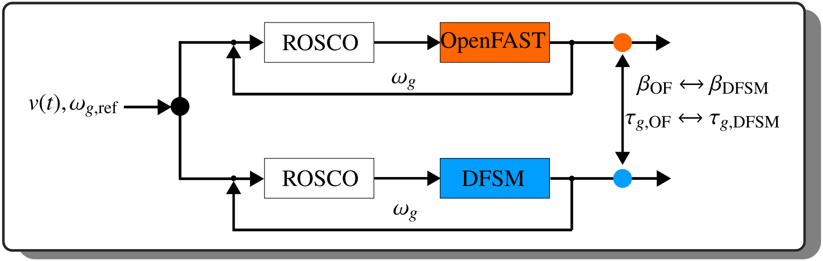

- ROSCO has been integrated with the DFSM approach to use the DFSM model as the plant model instead of OpenFAST
- Generator speed and its first-time derivative are the key states considered

$$\boldsymbol{\xi} = [\omega_g, \dot{\omega}_g], \dot{\boldsymbol{\xi}} = [\dot{\omega}_g, \ddot{\omega}_g]$$

- Current speed (v) is the only input
- The controls are still $\boldsymbol{u} = [\tau_g, \beta]$
- The generator power (P) and tower base moment (T_M) are the key outputs
- The low-fidelity linear model is used as the DFSM model

→ Results for the Transition Region

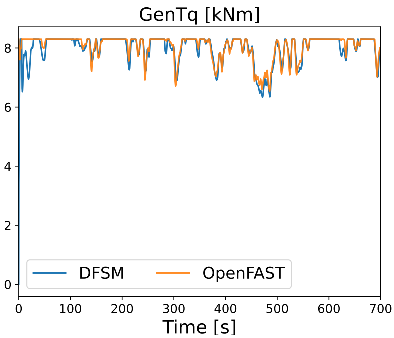

(a) Generator Torque.

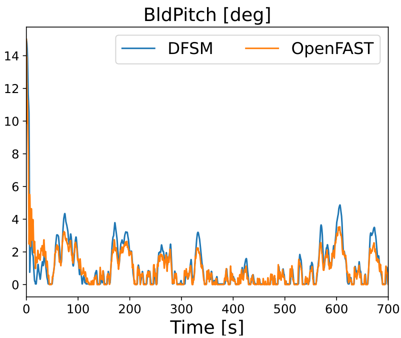

(b) Blade Pitch.

OpenFAST simulation time: 17 hours, **DFSM simulation time**: 67 sec, **Speedup**: 900×

→ Results for the Transition Region (cont.)

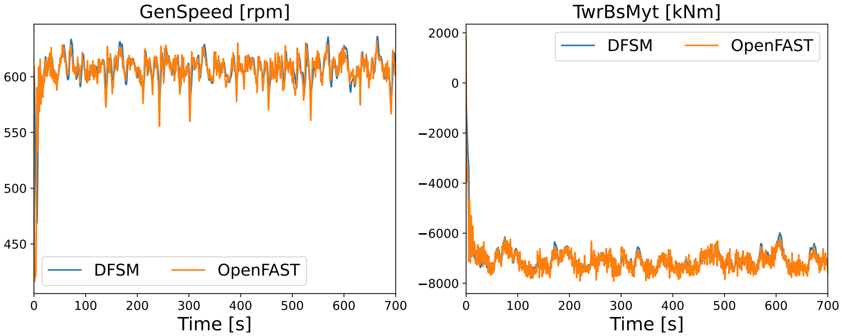

(a) Generator Speed. (b) Tower-Base Moment.

OpenFAST simulation time: 17 hours, **DFSM simulation time**: 67 sec, **Speedup**: 900×

→ Conclusion

- As part of the first study, ROSCO has been extended for control of marine turbines
- As part of the second study, a DFSM approach has been developed and validated for both wind and marine turbines
- The application of the DFSM for open-loop optimal control and closed-loop control using ROSCO has been demonstrated
- Utilizing the tools developed as part of these tasks to answer the research questions will be discussed briefly next

6

Future work

→ RQ1 CCD of Marine Turbines Using DFSM

RQ1 Using the DFSM approach and CCD, identify pathways that could result in a large reduction in the LCOE of floating marine turbine systems

- The goal of this study is to show the efficacy of the CCD for the design of marine turbines and demonstrate the use of the DFSM approach and the WEIS toolbox for the design of marine turbines

1. Identify a set of design variables belonging to the platform, mooring, tower subsystems
2. Identify key design driving DLCs for marine turbines
3. Find the optimal design of the floating marine turbine through a sequential approach to minimize the LCOE
    - This will be the benchmark value
4. Identify the optimal design using CCD with the nested approach:
    - For each iteration of the outer loop, construct the DFSM model
    - Solve an open-loop optimal control problem to maximize the annual energy production (AEP) and minimize the tower-base loads
    - Calculate the LCOE value
    - Repeat till convergence
5. Compare the LCOE, AEP, key tower and blade loads for the sequentially designed turbine and the optimal design obtained using CCD

→ RQ2 Identifying Platform Trade-Offs for FOWTs using CCD

RQ2 Identify the trade-offs between different platform designs for FOWTs using CCD

1. Identify a set of design variables belonging to the platform, mooring, and tower subsystems for the three different types of platforms
   - Semisubmersible, spar buoy, tension leg
2. Identify the optimal design for each platform type using CCD with the nested approach:
   - For each iteration of the outer loop, construct the DFSM model
   - Solve an open-loop optimal control problem to maximize the annual energy production (AEP) and minimize the tower-base and blade loads
   - Calculate the LCOE value
   - Repeat till convergence
3. Compare the LCOE, AEP, key tower and blade loads for the optimized designs of all three platform types for different locations, and identify the trade-offs

→ RQ3 Open-Loop to Closed-Loop Optimal Control

RQ3 Identify approaches to construct closed-loop optimal controllers based on the insights identified using open-loop optimal control trajectories

1. **Trajectory tracking approach:** Set up the closed-loop controller to follow the open-loop trajectory
2. **Performance tracking approach:** Set up the closed-loop controller to have the same mean and standard deviation of key objectives as the open-loop optimal control solutions

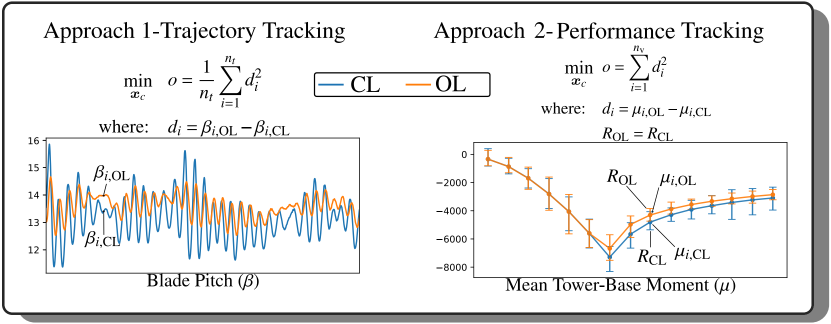

→ RQ3 Open-Loop to Closed-Loop Optimal Control (cont.)

- Generate different (n_{seeds}) wind/current input profiles for different wind/current speeds (n_v), each having n_t points
- Generate DFSM model
- Solve the open-loop optimal control problem for all $n_v \times n_{\text{seeds}}$ and generate optimal trajectories

- **Approach 1**
- Generate representative trajectory for each n_v wind speed, by aggregating the results of n_{seeds}
- Solve a closed-loop optimal control problem for the representative set of wind/current profiles to get $\boldsymbol{x}_c$ such that the mean square error between the aggregated open-loop solution and closed-loop solution, $\boldsymbol{u}_{\text{OL}}$ and $\boldsymbol{u}_{\text{CL}}$, is minimized

- **Approach 2**
- Find the mean (μ) and range (R) of a given objective, say the tower base moment T_M, for each wind/current speed n_v across the different n_{seeds} for the open-loop optimal control solution
- Solve a closed-loop optimal control problem for the same set of $(n_v \times n_{\text{seeds}})$ wind/current profiles to get $\boldsymbol{x}_c$ such that the squared error between the mean of the open-loop solution (μ_{OL}) and closed loop solution (μ_{CL}), is minimized

- Compare the performance of each controller for a new set of wind/current profiles and compare the results

→ References

- N. J. Abbas, J. Jasa, et al. (2024). "Control co-design of a floating offshore wind turbine". *Applied Energy* 353. doi: 10.1016/j.apenergy.2023.122036. ISSN: 0306-2619
- N. J. Abbas, D. Zalkind, et al. (2022). "A reference open-source controller for fixed and floating offshore wind turbines". *Wind Energy Sci.* 7.1. doi: 10.5194/wes-7-53-2022
- J. T. Allison, T. Guo, and Z. Han (2014). "Co-Design of an active suspension using simultaneous dynamic optimization". *J. Mech. Design* 136.8. doi: 10.1115/1.4027335. DOI: 10.1115/1.4027335
- S. Bayat, Y. H. Lee, and J. T. Allison (2023). "Nested Control Co-design of a Spar Buoy Horizontal-axis Floating Offshore Wind Turbine". arXiv: 2310.15463 [eess.SY]
- S. Butterfield et al. (2007). "Engineering Challenges for Floating Offshore Wind Turbines". *Copenhagen Offshore Wind Conference*. url: https://www.osti.gov/biblio/917212
- A. P. Deshmukh and J. T. Allison (2017). "Design of Dynamic Systems Using Surrogate Models of Derivative Functions". *J. Mech. Design* 139.10. doi: 10.1115/1.4037407
- T. Dewhurst et al. (2013). "Dynamics of a Floating Platform Mounting a Hydrokinetic Turbine". *Mar. Technol. Soc. J.* 47.4. doi: 10.4031/mtsj.47.4.13
- P. L. Fraenkel (2002). "Power from marine currents". *Proceedings of the Institution of Mechanical Engineers, Part A: Journal of Power and Energy* 216.1. doi: 10.1243/09576500276002
- G. F. Franklin, J. D. Powell, and A. Emami-Naeini (2015). *Feedback control of dynamic systems*. Vol. 33. Pearson London
- M. Garcia-Sanz (2019a). "A Metric Space with LCOE Isolines for Research Guidance in wind and hydrokinetic energy systems". *Wind Energy* 23.2. doi: 10.1002/we.2429

→ References (Continued)

- M. Garcia-Sanz (2019b). "Control Co-Design: An engineering game changer". *Adv. Control Appl.* 1.1. doi: 10.1002/adc2.18
- T. Gunnink (2015). "Analysis and Regulation of the Coupled Dynamics of a Two- Turbine Floating Tidal Energy Converter". https://repository.tudelft.nl/islandora/object/uuid%3A4670bb38-ffbb-44c1-86ac-0d6498d9433f?collection=education. M.S. Thesis. Delft University of Technology
- X. Guo et al. (2018). "Dynamic responses of a floating tidal turbine with 6-DOF prescribed floater motions". *Ocean Engineering* 165. doi: 10.1016/j.oceaneng.2018.07.017
- T. de Jesus Henriques et al. (2014). "The effects of wave–current interaction on the performance of a model horizontal axis tidal turbine". *Int. J. Mar. Energy* 8. doi: 10.1016/j.ijome.2014
- J. M. Jonkman and D. Matha (2011). "Dynamics of offshore floating wind turbines—analysis of three concepts". *Wind Energy* 14.4. doi: 10.1002/we.442. ISSN: 1099-1824
- J. Jonkman (2008). "Influence of Control on the Pitch Damping of a Floating Wind Turbine". *46th AIAA Aerospace Sciences Meeting and Exhibit*. doi: 10.2514/6.2008-1306. American Institute of Aeronautics and Astronautics
- J. Jonkman et al. (2021). "Functional Requirements for the WEIS Toolset to Enable Controls Co-Design of Floating Offshore Wind Turbines". *ASME 2021 International Offshore Wind Technical Conference*. doi: 10.1115/iowtc2021-3533
- T. Lefebvre, F. D. Belie, and G. Crevecoeur (2018). "A trajectory-based sampling strategy for sequentially refined metamodel management of metamodel-based dynamic optimization in mechatronics". *Optim. Control Appl. Methods* 39.5. doi: 10.1002/oca.2442

→ References (Continued)

- R. Martinez et al. (2020). "Analysis of the effects of control strategies and wave climates on the loading and performance of a laboratory scale horizontal axis tidal turbine". *Ocean Engineering* 212. doi: 10.1016/j.oceaneng.2020.107713
- X. Mei and M. Xiong (2021). "Effects of Second-Order Hydrodynamics on the Dynamic Responses and Fatigue Damage of a 15 MW Floating Offshore Wind Turbine". *Journal of Marine Science and Engineering* 9.11. doi: 10.3390/jmse9111232. ISSN: 2077-1312
- R. E. Murray, R. Thresher, and J. Jonkman (2018). "Added-mass effects on a horizontal-axis tidal turbine using FAST v8". *Renewable Energy* 126. doi: 10.1016/j.renene.2018.04.023
- *OpenFAST* (n.d.). [Online,48b0ae6]. url: https://github.com/OpenFAST/openfast/tree/dev
- S. Ordonez-Sanchez et al. (2019). "Analysis of a Horizontal-Axis Tidal Turbine Performance in the Presence of Regular and Irregular Waves Using Two Control Strategies". *Energies* 12.3. doi: 10.3390/en12030367
- L. Y. Pao et al. (2021). "Control co-design of 13 MW downwind two-bladed rotors to achieve 25% reduction in levelized cost of wind energy". *Annu. Rev. Control* 51. doi: 10.1016/j.arcontrol.2
- H. Ross et al. (2022). "Development of a Control Co-Design Modeling Tool for Marine Hydrokinetic Turbines". *ASME 2023 International Mechanical Engineering Congress & Exposition*. doi: 10.1115/imece2022-94483
- A. K. Sundarrajan, W. W. Daniel R. Herber, et al. (2024). "Development of an optimal variable pitch controller for floating axial-flow marine hydrokinetic turbines". *(submitted to) American Control Conference*

→ References (Continued)

- A. K. Sundarrajan, Y. Hoon Lee, et al. (2023). "Open-Loop Control Co-Design of Semisubmersible Floating Offshore Wind Turbines Using Linear Parameter-Varying Models". *Journal of Mechanical Design* 146.4. doi: 10.1115/1.4063969. ISSN: 1528-9001
- A. K. Sundarrajan and D. R. Herber (2023). "Using High-fidelity Time-Domain Simulation Data to Construct Multi-fidelity State Derivative Function Surrogate Models for use in Control and Optimization". eprint: 2308.07419 (eess.SY)
- S. Tatum et al. (2016). "Wave–current interaction effects on tidal stream turbine performance and loading characteristics". *Int. Mar. Energy J.* 14. doi: 10.1016/j.ijome.2015.09.002
- K. P. Thiagarajan and H. J. Dagher (2014). "A review of floating platform concepts for offshore wind energy generation". *J. Offshore Mech. Arct. Eng.* 136.2. doi: 10.1115/1.4026607. DOI: 10.1115/1.4026607
- D. Zalkind et al. (2022). "Floating wind turbine control optimization". *Journal of Physics: Conference Series* 2265.4. doi: 10.1088/1742-6596/2265/4/042021
- L. Zhang et al. (2015). "The effects of surge motion of the floating platform on hydrodynamics performance of horizontal-axis tidal current turbine". *Renewable Energy* 74. doi: 10.1016/j.renene.2014.09.002
- Q. Zhang, Y. Wu, and L. Lu (2022). "A Novel Surrogate Model-Based Solving Framework for the Black-Box Dynamic Co-Design and Optimization Problem in the Dynamic System". *Mathematics* 10.18. doi: 10.3390/math10183239

Questions?

Optimal Control and Control Co-Design of Wind and Marine Turbines Using Derivative Function Surrogate Models

Fort Collins

December 14, 2023

Athul Krishna Sundarrajan

Colorado State University

Athul.Sundarrajan@colostate.edu

PhD Timeline- Gantt Chart

WEIS

Appendix

→ Open-Loop Optimal Control

Initial Exploratory Study

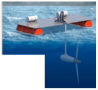

- A simple LSTM network was implemented to approximate the state derivatives given states and controls for a floating offshore wind turbine
- Time series simulation for 1300 s was obtained using WEIS
- The dataset is sequentially partitioned into two data sets: training and validation
  - Training for 40% of the horizon, Validation for 60% the remaining portion
- A shallow neural network is not well suited to capture the complex dynamic information from OpenFAST
- Since we are working with time series data, a type of recurrent neural network (RNN) called long short-term memory (LSTM) networks are more suited
  - LSTM networks can keep track of long-term dependencies between time steps of data
- Recent studies have shown RNN, and LSTM networks can be used to approximate the input-output response of nonlinear dynamic systems: Paper 1, Paper 2
  - A recent study has shown that LSTMs can approximate unsteady aerodynamic response of wind turbines using OpenFAST: Link

$$\boldsymbol{\xi} = [\Theta_p, \omega_g, d\Theta_p, d\omega_s] \quad : \text{States}$$

$$\boldsymbol{u} = [w, \tau_g, \beta] \quad : \text{Controls}$$

$$\dot{\boldsymbol{\xi}} = [d\Theta_p, d\omega_g, d^2\Theta_p, d^2\omega_s] \quad : \text{State Derivatives}$$

$$\dot{\boldsymbol{\xi}} \approx f_{\text{DFSM}}(\boldsymbol{\xi}, \boldsymbol{u})$$

Quantities considered

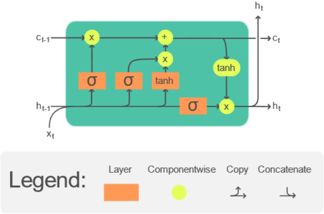

LSTM architecture (source : wikipedia)

→ Additional Results

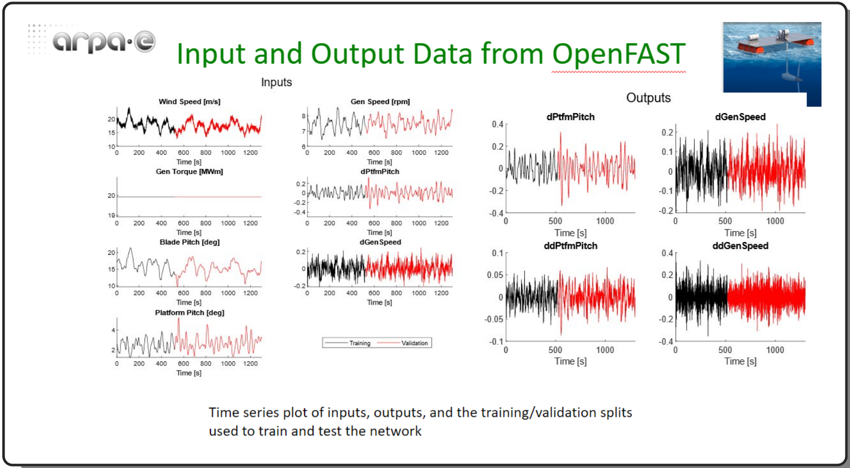

→ Additional Results (continued)

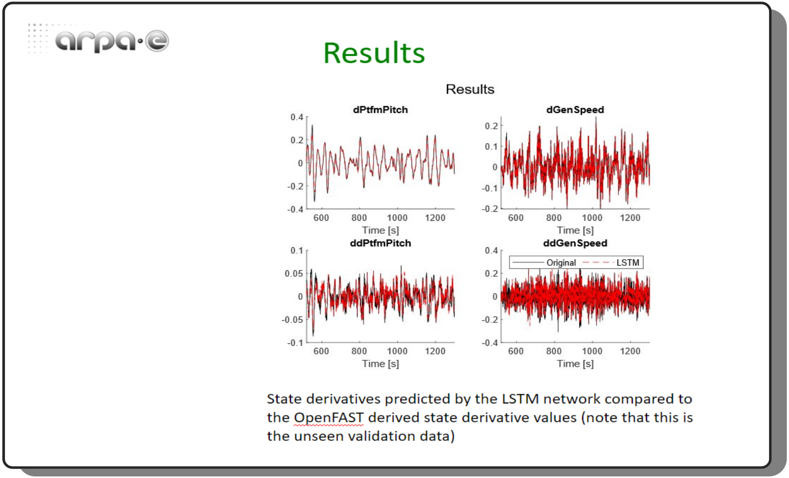

→ Results for Marine Turbine

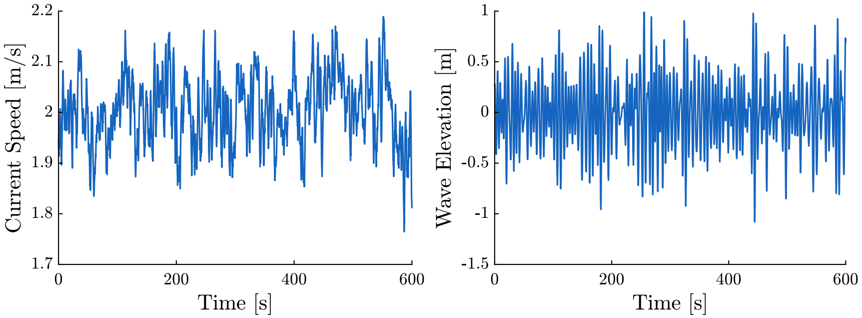

(a) Generator Speed. (b) Platform Pitch.

- We use the RM1 marine turbine model with a semi-submersible platform
- The same states are used, whereas the inputs are current speed and wave elevation
- System simulations are obtained for ten different trajectories from DLC 1.1
- A GPR-based error corrective function is used in this case
- 40% are used to train the DFSM model, and the rest are used for testing

→ Validation Results

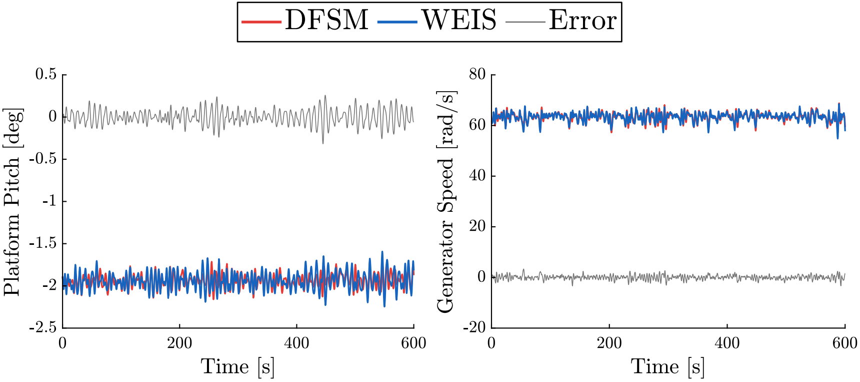

(a) Current Speed.   (b) Wave Elevation.

WEIS simulation time: 17 hours, **DFSM simulation time**: 15 sec,
Speedup: 4000×

→ Validation Results (Continued)

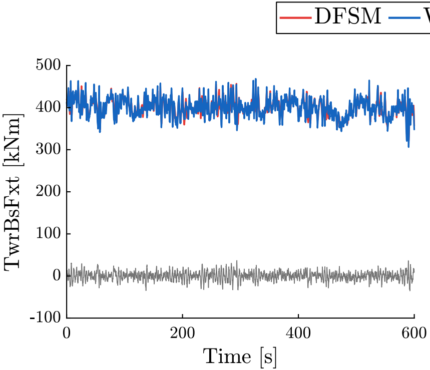

(a) Tower-base share force.

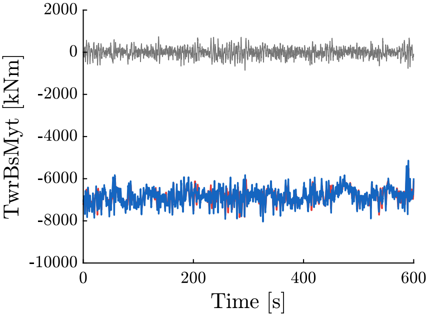

(b) Tower-base shear moment.

→ Validation Results (Continued)

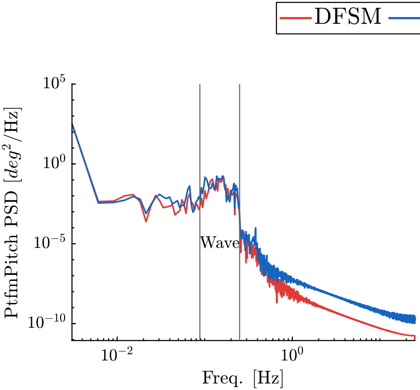

(a) PSD of platform pitch.

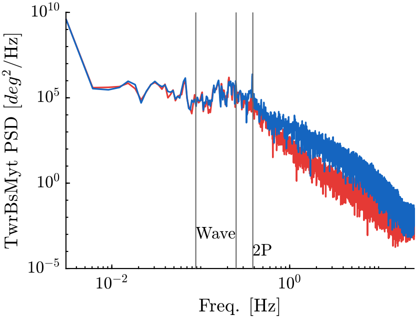

(b) PSD of tower-base shear moment.

→ ROSCO Results for Below-Rated Region

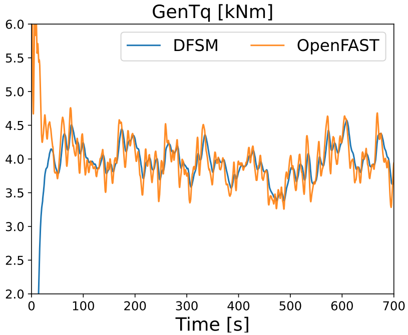

(a) Generator Torque.

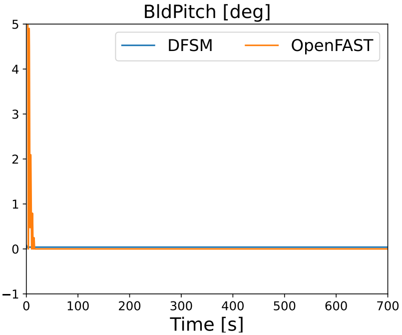

(b) Blade Pitch.

OpenFAST simulation time: 17 hours, **DFSM simulation time**: 20 sec, **Speedup**: 3000×

→ Results for Above-Rated Region

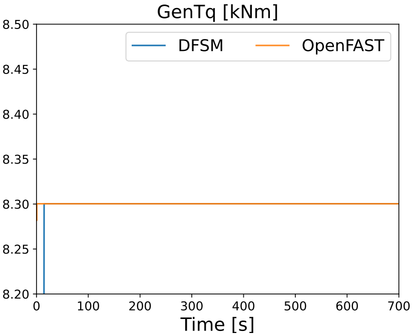

(a) Generator Torque.

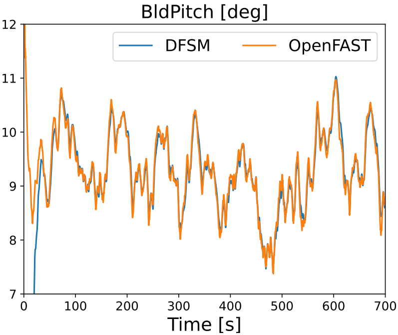

(b) Blade Pitch.

OpenFAST simulation time: 17 hours, **DFSM simulation time**: 60 sec, **Speedup**: 1000×